SHELX-76 program[36] by using full-matrix least-squares techniques of F_o, minimizing the function $\sum w(|F_o| - |F_c|)^2$.

[(Cp*Ru)$_2$(η^6,η^6-PhC≡CPh)](CF$_3$SO$_3$)$_2$ (6). All non-hydrogen atoms were refined anisotropically. All H atoms were observed but introduced in calculations in constrained geometry (C–H = 0.97 Å) with a general isotropic temperature factor, first refined, and then kept fixd to 0.06 Å. The refinement converged to R = 0.030 and R_w = 0.037 with a maximum shift/esd of 0.010 on the final cycle (mean value: 0.003) with 235 variable parameters. A fit of S = 1.19 for the data using the weighting scheme $w = [\sigma^2(F_o) + 0.0004F_o^2]^{-1}$ was obtained. The maximum residual peak was near the Ru atom at 0.7 e/Å^3. Fractional atomic coordinates are given in Table VIII.

0.7{[Cp*Ru(PhCOO)]·2H$_2$O}0.3{[Cp*Ru(PhCOOCH$_3$)]OH} (15′). All non-hydrogen atoms of the [Cp*Ru(PhCOO)] entity were refined anisotropically. The two important residuals were first considered as water molecules and refined so. The subsequent difference-Fourier showed unambiguously H atoms of the Cp* and Ph groups, which were introduced in calculations with constrained geometry (C–H = 0.97 Å) with general isotropic temperature factors, first refined, and then kept fixed to 0.11 and 0.042 Å^2, respectively. Near the Ow(1) atom, two H atoms could be located, one of them being clearly at a lower height than the other one. Near the Ow(2) atom, there was a residual of about 1.8 e/Å^3 that could not be attributed to one H atom only. After distance calculations and chemical experiments, it appeared that the most suitable explanation was a disorder between a methyl and a water molecule. Occupancy factors of Ow(2) and C(18) methyl carbon were refined and then kept fixed to 0.70 and 0.30, respectively. Ow(2) was refined anisotropically, C(18) isotropically. No H atom was introduced on these two atoms. The H atoms near Ow(1) were refined, first with occupancy factors 1.0 and free isotropic thermal parameters. To obtain the same U value of 0.11 Å^2, occupancy factors were 1.0 for H1(w1) and 0.7 for H2(w1). It may be assumed that the 70% Ow(1) water molecule and the 30% OH^- anion are not discernible. Ow(1) was refined anisotropically. It is noteworthy that the U_{11} component of Ow(1) and Ow(2) atoms is higher than the other two. The refinement converged to R = 0.032 and R_w = 0.042 with a maximum shift/esd of 0.113 (a H parameter) on the final cycle (mean value 0.007) with 209 variable parameters. A fit of $_S$ = 1.15 for the data using the weighting scheme $w = [\sigma^2(F_o) + 0.00035F_o^2]^{-1}$ was obtained. The maximum residual peak was between the Ow(2) and C(18) atoms at 0.8 e/Å^3. Fractional atomic coordinates are given in Table IX.

[Ru$_2$(Cp*)$_2$(PhC$_2$H)$_2$(MeCN)](CF$_3$SO$_3$) (18). Cp* and Ph rings were refined as isotropic rigid groups (C–C = 1.420 and 1.395 Å, respectively). All other non-hydrogen atoms were refined anisotropically, the occupancy factors of the two CF_3SO_3 entities having been first refined and then kept fixed to 0.5. All H atoms were introduced in calculated positions (C–H = 0.97 Å) with isotropic thermal parameters kept fixed to 0.07 Å^2 for methyl groups, 0.065 Å^2 for phenyl groups, and 0.05 Å^2 for C_2H_2 groups. Both enantiomers were tested and the best one kept (Hamilton test,[37] R-factor ratio = 1.08, significance level α = 0.01). The refinement converged to R = 0.036 and R_w = 0.038 with a maximum shift/esd of 0.08 (a F thermal parameter) on the final cycle (mean value 0.009) with 361 variable parameters. A fit of S = 1.22 for the data using the weighting scheme $w = [\sigma^2(F_o) + 0.0018F_o^2]^{-1}$ was obtained. The maximum residual peak was near the C(20) atom at 0.4 e/Å^3. Fractional atomic coordinates are given in Table X.

Supplementary Material Available: Tables listing fractional and hydrogen atomic coordinates, equivalent temperature factors, thermal parameters, and bond lengths and angles for compounds listed in the text (20 pages); tables listing observed and calculated structure factors (40 pages). Ordering information is given on any current masthead page.

(36) Sheldrick, G. M. SHELX 76, Program for Crystal Structure Determination; University of Cambridge, England, 1976.

(37) In ref 33, p 288.

Cyclopentadienyl(allyl)(butadiene)hafnium Compounds. Synthesis, Crystal Structure, and Dynamics of Cyclopentadienyl(1,2,3-trimethylallyl)(1,2-dimethylbutadiene)-hafnium and Cyclopentadienyl(1,1,2-trimethylallyl)-(2,3-dimethylbutadiene)hafnium

Thomas J. Prins, Bryan E. Hauger, Peter J. Vance, Michael E. Wemple, David A. Kort, Jonathan P. O'Brien, and Michael E. Silver*

Department of Chemistry, Hope College, Holland, Michigan 49423

John C. Huffman

Department of Chemistry, Indiana University, Bloomington, Indiana 47405

Received July 19, 1990

The reaction of CpHfCl$_3$·2THF with 2 equiv of (1,2,3-Me$_3$allyl)MgBr or (1,1,2-Me$_3$allyl)MgBr yields Cp(1,2,3-Me$_3$allyl)(1,2-Me$_2$butadiene)Hf (**3**) or Cp(1,1,2-Me$_3$allyl)(2,3-Me$_2$butadiene)Hf (**4**). X-ray crystallography of **3** shows that both the allyl and butadiene ligands assume a prone orientation with respect to Cp. For **3**: cell constants a = 15.109 (5), b = 7.150 (2), c = 15.587 (6) Å, β = 115.41 (1)°; space group $P2_1/c$; R = 0.0305, R_w = 0.0347. Variable-temperature ^{1}H NMR studies indicate that compound **3** is static on the NMR time scale whereas **4** exists in two isomeric forms and undergoes three separate dynamic processes involving η^3–η^1 isomerization at the unsubstituted and substituted ends of the allyl ligand [ΔG^* = 39.4 ± 1.0 kJ/mol and 73.4 ± 1.0 kJ/mol, respectively] and butadiene flip [ΔG^*(avg) = 49.8 ± 1.0 kJ/mol].

Introduction

Early transition metal compounds possessing allyl and/or butadiene ligands differ substantially from those whose only π ligand is cyclopentadienide (Cp). Allyl and butadiene ligands provide low barriers for a number of dynamic processes[1-3] and decomposition routes[4,5] not

0276-7333/91/2310-0979$02.50/0

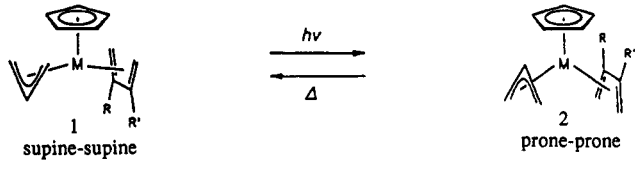

a M = Zr, R = R' = H
b M = Zr, R = H, R' = CH_3
c M = Zr, R = R' = CH_3
d M = Zr, R = H, R' = Ph
e M = Hf, R = R' = H

Figure 1. CpM(allyl)(butadiene) [M = Zr, Hf] compounds prepared by Erker et al.[6]

available to Cp compounds. For example, Erker and coworkers have studied the CpM(allyl)(butadiene) complexes shown in Figure 1.[6] All of the compounds exist in a supine–supine ground state but can be photoisomerized to a higher energy prone–prone configuration. On the basis of extended Huckel calculations, Erker postulates that the photoisomerization occurs via a *simultaneous* flip of the butadiene ligand and rotation of the η^3-allyl ligand about its centroid. Conclusive experimental support for this is not possible since the only process observed via NMR upon warming is the dissapearance of the signals due to **2** and the growth of those due to **1**.

We have been studying the effect of extensive ligand methylation on the structure, dynamics, and reactivity of early transition metal allyl and butadiene compounds. We have previously demonstrated that both the number and position of methyl substituents on an allyl ligand can have a dramatic effect on how it binds to Cp_2ZrBr[7] and Cp^*ZrBr_2[3] moieties ($Cp^* = C_5Me_5$) and on the barrier to η^3–η^1 allyl rearrangement. In this paper we will show that the same is true for the allyl and butadiene ligands of CpHf(allyl)(butadiene) complexes. We report here on the preparation of Cp(1,2,3-Me_3allyl)(1,2-Me_2butadiene)Hf (**3**) and Cp(1,1,2-Me_3allyl)(2,3-Me_2butadiene)Hf (**4**), the X-ray structural characterization of **3**, and the dynamic behavior of **4**. Unlike complexes **1** and **2**, compound **4** exhibits two isomeric forms at all temperatures and three separate dynamic processes, allowing for experimental confirmation of the rearrangement mechanisms involved.

Experimental Section

General Comments. Ether, hexane, and pentane were distilled from sodium/benzophenone under argon. The bromo allyls (1,2,3-trimethylallyl bromide and 1,1,2-trimethylallyl bromide) used to prepare the allyl Grignards were prepared as described elsewhere.[8] The ether solutions of the allyl Grignards (1,2,3-Me_3allyl)MgBr and (1,1,2-Me_3allyl)MgBr were prepared as described previously (with the modification that (1,2,3-Me_3allyl)MgBr was prepared in diethyl ether).[3] $CpHfCl_3$·2THF was prepared described elsewhere.[9] Hafnium tetrachloride was purchased from the Aldrich Chemical Co. and used without further purification. All syntheses and subsequent handling of compounds were conducted in a dry box under a dry argon atmosphere.

CpHf(1,2,3-Me_3allyl)(1,2-Me_3butadiene) (3). At 0 °C an ether solution of (1,2,3-Me_3allyl)MgBr (0.0320 M, 265 mL, 8.48 mmol) was added dropwise to a stirred slurry of 2.05 g (4.15 mmol) $CpHfCl_3$·2THF in 100 mL of ether. The reaction solution turned pale yellow upon addition of the Grignard and was golden yellow by the end of the 1-h addition. Stirring was continued at 0 °C for 0.5 h. The cooling bath was then removed and 100 mL of hexane was added. The reaction solution was reduced in volume to ~250 mL via trap to trap distillation and 100 mL of hexane were again added. The solution volume was further reduced to ~100 mL during which time magnesium halide salts precipitated. The reaction solution was filtered, and the salts were washed with a small amount of pentane. The pentane wash was combined with the red-orange filtrate. The solvent was then removed via trap to trap distillation, yielding a red solid and a dark red oil. The oil was removed from the solid by pipet. The red solid was dissolved in 2 mL of pentane and cooled to −40 °C, yielding 0.20 g of red crystals. On standing the red oil yielded a second crop of red solid. The oil was again removed by pipet. The second crop of solid was washed with a small amount of cold pentane. The pentane wash was combined with the red oil yielding a dark red solution. The second crop of red solid was then dissolved in 2 mL of pentane and cooled to −40 °C, yielding 0.32 g of red crystals. The dark red solution was cooled to −40 °C, yielding an additional 0.10 g of red crystals. All three crops of red crystalline solid (0.62 g, 54%, mp 77.5–79.0 °C dec) were pure by NMR. ^{1}H NMR (THF-d_8/TMS 2%): δ 4.97 (Cp, 5 H); 4.91 t (CH, butadiene, 1 H); 2.92 t (CH, butadiene, exo, 1 H); 2.37 (CH_3, allyl, 3 H); 2.16 (CH_3, butadiene, 3 H); 2.04 d (CH_3, allyl, 3 H); 1.98 d (CH_3, butadiene, 3 H); 1.95 d (CH_3, allyl, 3 H); 1.60 m, br (CH, allyl, 1 H); 0.88 m, br (CH, allyl, 1 H); −1.44 t (CH, butadiene, endo, 1 H); −2.02 q (CH, butadiene, 1 H). Anal. Calcd for $C_{17}H_{26}Hf$: C, 49.94; H, 6.41; Hf, 43.65. Found: C, 49.79; H, 6.28; Hf, 43.73.

CpHf(1,1,2-Me_3allyl)(2,3-Me_2butadiene) (4). An ether solution of (1,1,2-Me_3allyl)MgBr (0.0264 M, 310 mL, 8.18 mmol) was added to a stirred slurry of 2.00 g (4.05 mmol) of $CpHfCl_3$·2THF in 20 mL of ether. The color of the reaction solution progressed from yellow to deep orange during the 1-h addition. After addition was complete 100 mL of hexane were added. The volume of the reaction solution was reduced by one half via trap-to-trap distillation in order to precipitate magnesium halide salts. The solution was filtered and the salts were washed twice with 20-mL portions of hexane. The washes were combined with the filtrate. The solvent was removed via trap-to-trap distillation, yielding an orange oil. This oil was washed three times with 30-mL portions of pentane, yielding an orange-red solution and insoluble salts. The solution was isolated by filtration. Concentration of the orange-red solution via trap-to-trap distillation and subsequent cooling to −40 °C caused precipitation of more salts. The solution was isolated and then concentrated to ~10 mL via trap-to-trap distillation. Cooling to −40 °C yielded a dark red-brown solid and oil. The oil was removed by pipet. The solid melted upon warming to room temperature. Both the melted solid and the dark oil were dissolved in a minimum amount of pentane and cooled to −40 °C. Both of these recrystallization attempts yielded dark red-brown solid. The solids were isolated and melted upon warming. The two crops were combined and recrystallized three times from minimum amounts of pentane. After each recrystallization the isolated solids melted at room temperature, although more slowly each time. The third recrystallization yielded dark red crystals which were weighed (0.36 g, 32%) before they melted. ^{1}H-NMR (toluene-d_8, 22 °C): δ 5.70 br (Cp, 5 H); 2.07 (CH_3, butadiene, 6 H); 1.92 (CH_3, allyl, terminal, 3 H); 1.69 br (CH_3, allyl, backbone, 3 H); 1.47 br (CH_3, allyl, terminal, 3 H); 0.56 v br (CH_2, allyl, 2 H). ^{1}H NMR (toluene-d_8, −94 °C, refer to Figure IV): δ 5.78 (Cp_{II}); 4.69 (Cp_I); 3.12 d (EXO_I, $J_{H,H}$ = 9.2 Hz); 3.00 (SYN/ANT_{II}); 2.76 d (EXO_I, $J_{H,H}$ = 9.2 Hz); 2.26 d (EXO_{II}, $J_{H,H}$ = 10.3 Hz); 2.09 ($Me_I^{A,T}$); 2.06 ($2xMe_{II}^{B}$); 2.04

(1) Erker, G.; Engel, K.; Korek, U.; Czisch, P.; Berke, H.; Caubere, P.; Vanderesse, R. *Organometallics* **1985**, *4*, 1531.
(2) Fryzuk, M. D.; Haddad, T. S.; Rettig, S. J. *Organometallics* **1989**, *8*, 1723.
(3) Larson, E. J.; Van Dort, P. C.; Dailey, J. S.; Lakanan, J. R.; Pederson, L. M.; Silver, M. E.; Huffman, J. C.; Russo, S. O. *Organometallics* **1987**, *6*, 2141.
(4) Hessen, B.; Spek, A. L.; Teuben, J. H. *Angew. Chem., Int. Ed. Engl.* **1988**, *8*, 1058.
(5) Berg, K.; Erker, G. *J. Organomet. Chem.* **1984**, *270*, C53.
(6) Sontag, C.; Berke, H.; Sarter, C.; Erker, G. *Helv. Chim. Acta* **1989**, *72*, 1676.
(7) Larson, E. J.; Van Dort, P. C.; Lakanen, J. R.; O'Neil, D. W.; Pederson, L. M.; McCandless, J. J.; Silver, M. E.; Russo, S. O.; Huffman, J. C. *Organometallics* **1988**, *7*, 1183.
(8) Van Zyl, C. M.; McKeeby, J. L.; Van Dort, P. C.; Larson, E. J.; Huffman, J. C.; Silver, M. E. *Inorg. Chim. Acta* **1987**, *133*, 289.
(9) Renaut, P.; Tainturier, G.; Gautheron, B. *J. Organomet. Chem.* **1978**, *148*, 35.

Table I. Summary of Crystal Data and Intensity Collection for Cp(1,2-Me_2butadiene)(1,2,3-Me_3allyl)Hf (3)

formula	$C_{17}H_{21}Hf$
a, Å	15.109 (5)
b, Å	7.150 (2)
c, Å	15.587 (6)
β, deg	115.41 (1)
V, Å^3	1520.84
Z	4
d, g cm^{-3}	4.281
space group	$P2_1/c$
cryst dimens, mm	0.15 × 0.14 × 0.11
temp, °C	−155
radiation	Mo Kα (λ = 0.71069 Å)
linear abs coeff, cm^{-1}	241.275
receiving aperture	3.0 × 4.0 mm; 22.5 cm from cryst
takeoff angle, deg	2.0
scan speed	8.0° in 2θ/min
bkdg counts	4 s at each end
2θ limits, deg	6–45
data collected	$+h, +k, \pm l$
unique data	1989
unique data with $F_o^2 > 2.33\sigma(F_o^2)$	1780
$R(F)$	0.0305
$R_w(F)$	0.0347

(Me_I^B); 1.96 (SYN/ANT$_{II}$); 1.94 (Me_{II}^A); 1.90 (Me_I^B); 1.80 (Me_I^A); 1.59 (2xMe_{II}^A); 0.86 ($Me_I^{A,T}$); 0.03 ([CH_2]$_{II}^A$); −0.71 d (ENDO$_{II}$, $J_{H,H}$ = 10.8 Hz); −1.15 d (ENDO$_I$, $J_{H,H}$ = 8.8 Hz); −1.57 d (ENDO$_I$, $J_{H,H}$ = 8.4 Hz). Anal. Calcd for $C_{17}H_{26}Hf$: C, 49.94; H, 6.41. Found: C, 49.40; H, 6.32.

Nuclear Magnetic Resonance Spectra. Proton chemical shifts were measured with a General Electric OMEGA GN-30 300-MHz spectrometer. Peak positions are reported as δ in parts per million relative to TMS at δ 0 for THF-d_8 solutions of **3** or relative to Dow Corning high vacuum silicone grease at δ 0.26 for toluene-d_8 solutions of **4** (the methyl signals for **3** were poorly resolved in ambient temperature ^{1}H NMR spectra measured in toluene-d_8). Temperatures, determined by a copper/constantan thermocouple in the probe assembly, are estimated to be accurate to ±1.0 °C. Peak assignments for the ambient temperature spectrum of **3** and the −94 °C spectrum of **4** were accomplished via the 2D-COSY technique.

X-ray Structural Determination. Pertinent data for the structure of **3** is in Table I. A crystal was mounted on a Picker computer-controlled four-circle diffractometer equipped with a Furnas monochromator (HOG crystal) and cooled by a gaseous nitrogen cooling system. A systematic search of a limited hemisphere of reciprocal space for **3** located a set of diffraction maxima with systematic absences consistent with the monoclinic space group $P2_1/c$. Subsequent solution and refinement of the structure confirmed this choice. Orientation matrices and accurate unit cell dimensions were determined at low temperature from least-square fits of 32 reflections (20° < 2θ < 30°). Intensity data were collected by using the $\theta/2\theta$ scan method; four standard reflections, monitored every 300 reflection measurements, showed only statistical fluctuations. No absorption correction was deemed necessary on the basis of examination of ψ scans for three reflections near χ = 90°. The structure was refined successfully without this correction. The intensities were corrected for Lorentz and polarization factors and scaled to give the numbers of independent F_{hkl} values for $I > 2.33\sigma(I)$ indicated in Table I.

The structure was solved by a combination of direct methods (MULTAN78) and Fourier techniques. All atoms, including hydrogens, were located. All non-hydrogen atoms were refined anisotropically and all hydrogen atoms were refined isotropically; refinements converged to values for the conventional R indices shown in Table I. The maximum residual in the final difference Fourier synthesis was 0.45 e/Å^3. The weighting scheme used in the final calculations was of the form $w = 1/\sigma F^2$. Scattering factors were taken from ref 10. The scattering factor for the Zr atom was corrected for the real and imaginary parts of anomalous dispersion by using values from ref 10. All computations were carried out on a 386 PC using programs described elsewhere.[11] The positional parameters and equivalent isotropic thermal parameters for the non-hydrogen atoms are listed in Table II, the atom-numbering scheme being shown in Figure 2. Anisotropic thermal parameters for the non-hydrogen atoms are listed in Table III (supplementary material), hydrogen-atom coordinates and isotropic thermal parameters in Table IV (supplementary material), and structure factors in Table V (supplementary material).

Table II. Coordinates (×10^4) and Equivalent Isotropic Temperature Factors for Cp(1,2,3-trimethylallyl)(1,2-dimethyl-1,3-butadiene)Hf[a] (3)

atom	x	y	z	B(eq), Å^2
Hf	7293.6 (2)	2389.5 (4)	2664.7 (2)	1.2
C1	8941 (6)	1117 (12)	3013 (6)	1.9
C2	8934 (6)	1296 (11)	3907 (6)	1.9
C3	8162 (6)	511 (12)	4036 (6)	1.7
C4	9690 (8)	1966 (14)	2734 (8)	2.8
C5	9659 (7)	2531 (12)	4673 (7)	2.6
C6	8062 (9)	410 (15)	4952 (8)	3.1
C7	6820 (6)	412 (12)	1379 (6)	1.7
C8	5931 (6)	1414 (11)	1166 (6)	1.8
C9	5566 (6)	1664 (12)	1843 (6)	2.1
C10	5994 (6)	961 (12)	2795 (6)	1.9
C11	7177 (8)	−115 (14)	642 (8)	2.7
C12	5477 (8)	2488 (13)	236 (7)	2.7
C13	7497 (7)	5508 (11)	2094 (6)	2.1
C14	6578 (7)	5503 (11)	2105 (6)	2.1
C15	6737 (6)	5380 (11)	3062 (6)	1.8
C16	7735 (6)	5353 (11)	3616 (6)	1.8
C17	8219 (6)	5440 (10)	3033 (6)	1.6

[a] Estimated standard deviations are given in parentheses. Equivalent isotropic thermal parameters are calculated by using the formula given by: Hamilton, W. C. *Acta Crystallogr.* **1959**, *12*, 609.

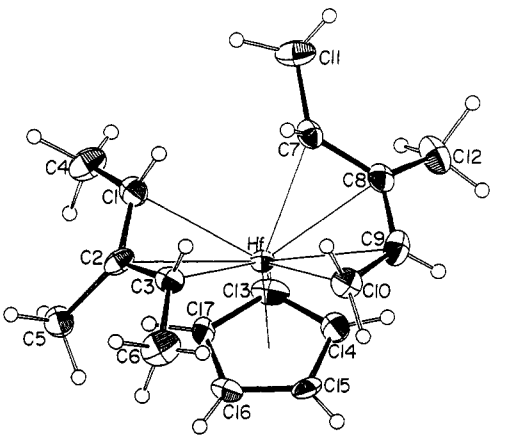

Figure 2. ORTEP diagram of Cp(1,2,3-Me_3allyl)(1,2-Me_2butadiene)Hf (3).

Results and Discussion

Synthesis of Hafnium Compounds. Solutions of the appropriate trimethylallyl Grignards in ether were added dropwise over 1 h to stirred ether slurries of $CpHfCl_3 \cdot 2THF$. Reaction of the metal halide with 2 equiv of allyl Grignard led to successful isolation of solid product upon removal of the solvent. Recrystallization from pentane yielded **3** and **4** as dark red crystalline solids, however, compound **4** melted when warmed to room temperature. Only compound **3** yielded crystals suitable for X-ray structure determination. Both compounds are highly air

(10) Ibers, J. A.; Hamilton, W. C., Eds. *International Tables for X-Ray Crystallography*; Kynoch: Birmingham, Engaldn, 1974; Vol. 4.

(11) Huffman, J. C.; Lewis, L. N.; Caulton, K. G. *Inorg. Chem.* **1980**, *19*, 2755.

Table VI. Bond Distances (Å) and Angles (deg) for Cp*(2,3-dimethylbutadiene)(1,1,2-trimethylallyl)Hf (3)

Bond Distances			
Hf–C1	2.481 (8)	C2–C3	1.384 (12)
Hf–C2	2.527 (8)	C2–C5	1.511 (12)
Hf–C3	2.384 (8)	C3–C6	1.501 (13)
Hf–C7	2.301 (8)	C7–C8	1.430 (12)
Hf–C8	2.460 (8)	C7–C11	1.512 (13)
Hf–C9	2.419 (a)	C8–C9	1.397 (12)
Hf–C10	2.299 (8)	C8–C12	1.519 (12)
Hf–C13	2.468 (8)	C9–C10	1.431 (12)
Hf–C14	2.465 (8)	C13–C14	1.396 (13)
Hf–C15	2.472 (8)	C13–C17	1.402 (12)
Hf–C16	2.507 (8)	C14–C15	1.408 (12)
Hf–C17	2.520 (7)	C15–C16	1.379 (12)
C1–C2	1.405 (12)	C16–C17	1.390 (12)
C1–C4	1.503 (13)		
Bond Angles			
C2–C1–C4	125.3 (8)	C9–C8–C12	119.5 (8)
C1–C2–C3	118.2 (8)	C8–C9–C10	126.2 (9)
C1–C2–C5	121.7 (8)	C14–C13–C17	108.6 (8)
C3–C2–C5	119.6 (8)	C13–C14–C15	107.1 (8)
C2–C3–C6	126.3 (8)	C14–C15–C16	107.9 (8)
C8–C7–C11	123.6 (8)	C15–C16–C17	109.3 (8)
C7–C8–C9	121.6 (8)	C13–C17–C16	107.0 (8)
C7–C8–C12	118.1 (8)		

sensitive and decomposed rapidly upon exposure to the atmosphere.

$$CpHfCl_3 \cdot 2THF + 2(allyl)MgBr \rightarrow \underset{3,4}{CpHf(butadiene)(allyl)} \quad (1)$$

	allyl	butadiene
3	1,2,3-Me_3allyl	1,2-Me_2butadiene
4	1,1,2-Me_3allyl	2,3-Me_2butadiene

Compounds 3 and 4 result from the thermal decomposition of tris-allyl intermediates which we did not isolate or attempt to characterize. It has been well established that Zr and Hf tris-allyl complexes of terminally methylated allyl ligands thermally decompose via intramolecular proton transfer to give butadiene–allyl compounds.[4,5] After the addition of 2 equiv of allyl Grignard to $CpHfCl_3 \cdot 2THF$ was complete the reaction solution was a bright orange color. During the course of additional stirring and workup the reaction solution turned to a darker red color. A reasonable explanation for this is initial formation of an orange tris-allyl intermediate which thermally decomposed to the dark red allyl-butadiene compound that was finally isolated. Although a two-to-one stoichiometry of allyl Grignard to $CpHfCl_3$ was used, it is likely that the initial product formed was predominantly $CpHf(allyl)_3$. We base this conclusion on our previous observation that reaction between equimolar amounts of allyl Grignard and Cp^*ZrCl_3 results in the initial formation of predominantly tris-substituted product.[3] The use of a two-to-one instead of a three-to-one stoichiometry (allyl Grignard to metal halide) was required for product isolation. A three-to-one ratio led to a dark red oil which would not yield a solid even though ^1H NMR showed it to contain a substantial amount of product.

Molecular Structure for 3. Final atomic coordinates and equivalent isotropic thermal parameters for the nonhydrogen atoms of 3 are presented in Table II; bond distances and angles are given in Table VI. A perspective view showing the molecular geometry and the atom numbering scheme is presented in Figure 2. In the monoclinic cell for 3 each molecule occupies a general position. The coordination geometry about Hf is essentially square pyramidal with an apical η^5-Cp ligand in which the η^3-allyl and the η^4-butadiene ligand both occupy basal positions. This geometry has also been observed for $CpZr(C_3H_5)(C_4H_6)$.[12]

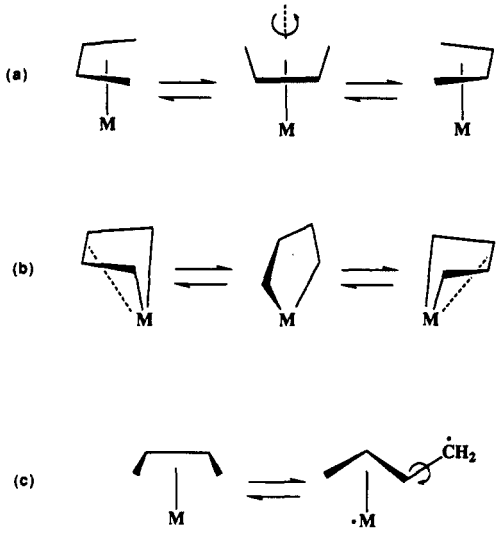

Figure 3. Fluxional processes for metal–diene complexes: (a) diene rotation about the metal-to-diene centroid axis; (b) envelope–flip mechanism; (c) slip mechanism. Only the latter two mechanisms can effect endo–exo exchange.

The normal to the Cp ligand plane is nearly colinear with the Hf–Ct(Cp) vector (angle of 1.8°). The η^3-allyl and η^4-butadiene ligands are both oriented in the prone configuration with respect to Cp. This is in contrast to $Cp(C_3H_5)(C_4H_6)Zr$ in which both the allyl and butadiene ligands assume a supine orientation.[12] Both ligands are tilted away from the Cp, the angle between the normal to the ligand plane and the Hf–Ct vector being 32.7° and 31.4° (allyl and butadiene, respectively). This minimizes repulsive contacts between ligand methyl groups and the Cp ring. Allyl: C4–C17, 0.205 Å; C5–C16, 0.364 Å; C5–C16, 0.410 Å. Butadiene: C12–C14, 0.273 Å. Values represent the amount that the nonbonded distance is within the sum of the van der Waals radii of a methyl group and an aromatic C–H group.[13] The tilt of the allyl and butadiene ligands results in longer Hf–C distances to the interior carbon atoms [Allyl: Hf–C2, 2.527 Å. Butadiene: Hf–C8, 2.460 Å; Hf–C9, 2.419 Å.] than to the exterior carbon atoms [Allyl: Hf–C1, 2.481 Å; Hf–C3, 2.384 Å. Butadiene: Hf–C7, 2.301; Hf–C10, 2.299 Å]. The Hf–C1 bond to the allyl ligand [2.481 Å] is 0.097 Å longer than the Hf–C3 bond [2.384 Å] at the other end, indicative of a slight distortion from an η^3 toward an η^1 binding mode. This distortion increases the distance between methyl groups C4 and C11 on the allyl and butadiene ligands to just beyond the sum of the van der Waals radii. Such distortion toward an η^1 mode in order to minimize repulsions between methyl groups has been observed for other cases.[3]

Isomers and Dynamic Behavior of Cp(1,1,2-Me_3allyl)(1,2-Me_2butadiene)Hf (4). The potential for dynamic behavior exists whenever a compound possesses either an η^3-allyl or an η^4-butadiene ligand. There are many examples of transition metal η^3-allyl complexes which undergo rearrangement via an η^1 transition state.[3,7,12,14-17] While the barrier for this rearrangement

(12) Erker, G.; Berg, K.; Kruger, C.; Muller, G.; Angermund, K.; Benn, R.; Schroth, G. *Angew. Chem., Int. Ed. Engl.* **1984**, *6*, 455.
(13) Pauling, L. *The Nature of the Chemical Bond*, 3rd ed.; Cornell University: Ithaca, NY, 1960; p 260. Pauling gives the van der Waals radius of a methyl group and an aromatic CH as 2.0 and 1.7 Å, respectively.
(14) (a) Faller, J. W. *Adv. Organomet. Chem.* **1977**, *16*, 211. (b) Tsutusi, M.; Courtney, A. *Adv. Organomet. Chem.* **1977**, *16*, 241.
(15) Faller, J. W.; Thomsen, M. E.; Mattina, M. J. *J. Am. Chem. Soc.* **1971**, *93*, 2642.

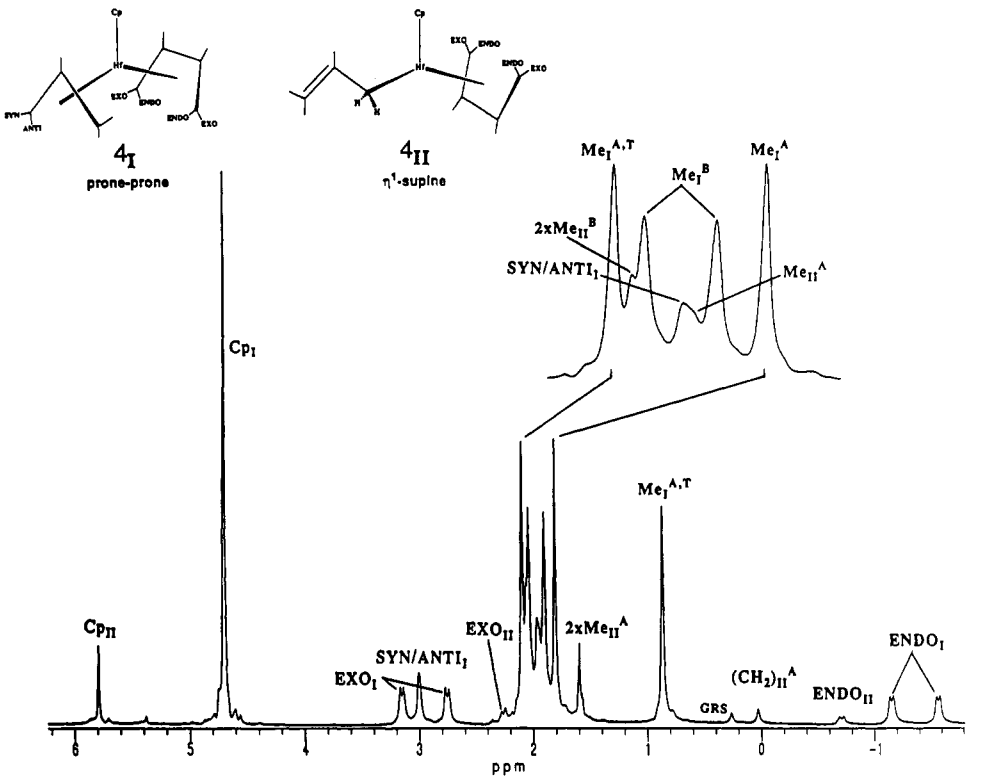

Figure 4. Isomers of Cp(1,1,2-Me_3allyl)(2,3-Me_2butadiene)Hf (4) along with ^1H NMR spectrum measured in toluene-d_8 at −94 °C. Peak positions and coupling constants are given in the Experimental Section. Subscripts I and II refer to isomers 4_I and 4_{II}. Superscripts A and B refer to the allyl and butadiene ligands, respectively. Superscript T refers to the terminal allyl positions (these two peaks coalesce at +95 °C). In the absence of these superscripts: $SYN/ANTI_I$ refers to the allyl protons in 4_I; EXO and ENDO refer to the butadiene CH_2 protons. GRS is silicone stopcock grease, used as a reference (δ 0.26). The peaks labled $SYN/ANTI_I$ are COSY correlated.

is a function of the ligand's environment, it is also strongly influenced by the pattern of ligand substitution.[3,15,16] For example, the rearrangement barrier ($\Delta G^{\ddagger}$) increases from 51.5 kJ/mol for Cp*(1,1,2-Me_3allyl)$ZrBr_2$ to 70.0 kJ/mol for Cp*(1,2,3-Me_3allyl)$ZrBr_2$.[16] This is primarily a steric effect, with substitution at the bound carbon increasing steric congestion in the η^1 transition state relative to the η^3 ground state. Likewise, η^4-butadiene ligands are also known to rearrange but via three different mechanisms (Figure 3). The η^4-butadiene ligand can (a) rotate about its M-to-centroid axis;[2] (b) envelope or diene flip via a metallacyclopentene transition state;[1,18,19] or (c) slip to an η^3-allyl binding mode with subsequent rotation about the uncoordinated C–C bond.[1] Rotation about the M-to-centroid axis may be distinguished from the flip and slip mechanisms since only the latter two can effect exchange of endo with exo substituents. The flip mechanism is not known for butadiene complexes in which the butadiene ligand is substituted at the terminal positions. Evidently, steric congestion that would be incurred at the metallacyclopentene transition state makes this mechanism unfavorable for terminally substituted butadienes.

In compound **3** the allyl ligand is substituted at both ends. As discussed, this would be expected to raise the barrier for η^3 to η^1 rearrangement. The butadiene ligand is substituted at one end. This would make rearrangement via the flip mechanism unlikely but should not have a large effect on the barrier to rearrangement via the rotation or slip mechanisms. However, ^1H NMR indicates that compound **3** remains static on the NMR time scale in toluene-d_8 up to 84 °C whereupon it suffers rapid decomposition. This implies that the rotation and slip mechanisms are also unfavorable for compounds of this type. The static behavior of **3** is in striking contrast to that of compound **4** which displays three separate dynamic processes and two different isomeric forms in toluene-d_8 solution. We will first discuss the isomeric forms and then the dynamic behavior.

Table VII. Calculated Destabilization (kJ/mol) Relative to the Most Stable Form[21]

allyl–butadiene orientation	$CpHf(C_3H_5)(C_4H_6)$	**4**
supine–supine	4.8	34.4
prone–prone	2.3	2.8
supine–prone	most stable	most stable
prone–supine	1.7	6.1

Figure 4 shows the two isomers postulated for compound **4** along with the ^1H NMR spectrum measured at −94 °C in toluene-d_8. Both isomers possess an η^4-*s-cis*-butadiene ligand. Endo proton resonances upfield of TMS (present for both isomers) are clear indicators of an *s-cis*-butadiene geometry as opposed to the far less common *s-trans* form.[5,19,20] The major isomer 4_I also has an η^3-bound allyl, indicated by the presence of separate resonances for syn and anti protons (correlated by 2D-COSY) as well as a unique upfield position for the syn methyl group.[3] Isomer 4_I gives rise to a Cp resonance at δ 4.69. Erker has shown that compounds of the type **2** (prone–prone) give rise to Cp

(16) Prins, T. J.; Hauger, B. E.; Vance, P. J.; Wemple, M. E.; Pederson, L. M.; Kort, D. A.; Kannisto, M. R.; Geerligs, S. J.; Kelly, R. S.; D. G. Peters; Huffman, J. C.; Silver, M. E., *Organometallics*, in press.
(17) Hauger, B. E.; Vance, P. J.; Prins, T. J.; Wemple, M. E.; Kort, D. A.; Kelly, R. S.; Huffman, J. C.; Silver, M. E. *Inorg. Chim. Acta*, in press.
(18) Spielvogel, B. F.; Das, M. K.; McPhail, A. T.; Onan, K. D.; Hall, I. H. *J. Am. Chem. soc.* **1980**, *102*, 6344.
(19) Erker, G.; Kruger, C.; Muller, G. *Adv. Organomet. Chem.* **1985**, *24*, 1.
(20) Dorf, U.; Engel, K.; Erker, G. *Organometallics* **1983**, *2*, 462.

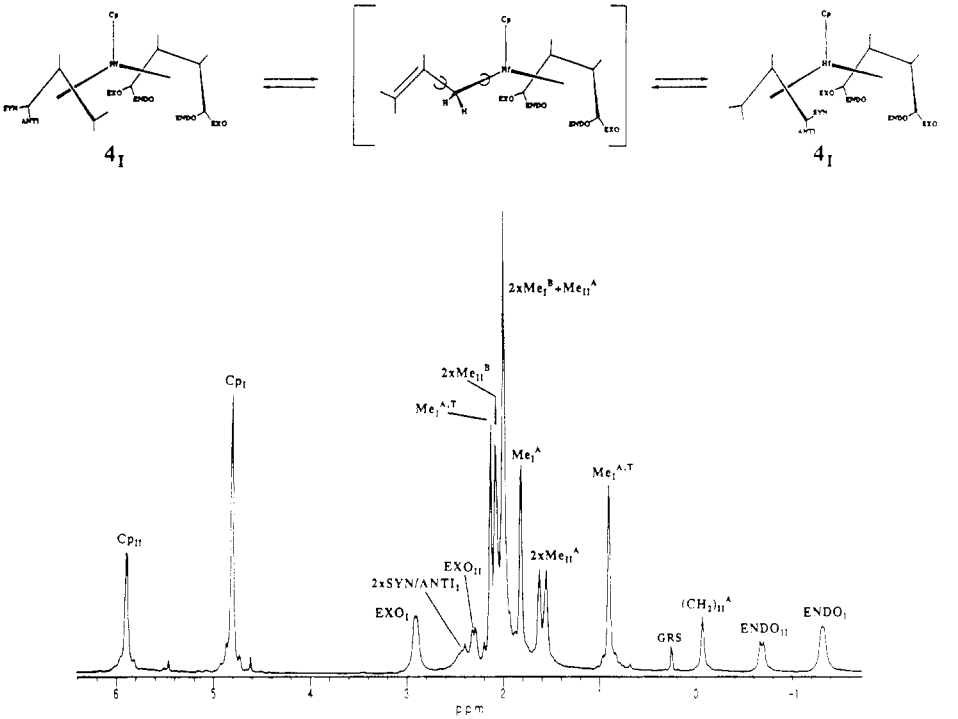

Figure 5. Lowest barrier dynamic process for 4_I, responsible for equilibrating the butadiene exo protons, butadiene endo protons, butadiene methyls and allyl syn/anti protons that were inequivalent at −94 °C (Figure 4). The ^{1}H NMR spectrum shown above was measured in toluene-d_8 at −49 °C (see Figure 4 caption for key to subscripts and superscripts). The signals due to 4_{II} are essentially unaffected by this process.

resonances between δ 4.45–4.61 in toluene-d_8.[6] Consistent with this, we have assigned the major isomer 4_I a prone–prone configuration. This is identical with the solid-state structure that we observed for **3**. Isomer 4_{II} is the minor isomer at this temperature ($4_I/4_{II}$ = 11.8/1.0 from area of the Cp peaks). Erker has shown that compounds of the type **2** (supine–supine) yield Cp signals between δ 6.02–6.11 in toluene-d_8. Isomer 4_{II} gives rise to a Cp resonance at δ 5.78. While this is close to Erker's range, we do not assign a supine–supine configuration to 4_{II}. In contrast to compounds of the type **1** and **2** [represented by CpHf(C_3H_5)(C_4H_6) in Table VII], molecular mechanics calculations show that the ligand methylation in **4** would essentially prohibit the supine–supine orientation and greatly favor all other orientations over it (Table VII).[21] In fact, examination of the spectrum in Figure 4 reveals that the allyl ligand is bound η^1 in 4_{II}. The η^1 orientation for the allyl ligand in 4_{II} is supported by noting that this minor isomer exhibits equivalent butadiene-endo, exo, methyl and allyl-CH_2 protons. Such equivalency could be brought about two ways: (1) via a molecular mirror plane containing all the carbon atoms of an η^1-allyl ligand, or (2) rapid η^3–η^1 allyl isomerization at the unsubstituted allyl carbon atom. Since 4_I is static on the NMR time scale at this temperature, it is unreasonable to argue that 4_{II} is fluxional. Therefore, 4_{II} must possess an η^1-allyl ligand. That the orientation of the butadiene ligand in 4_{II} is supine, opposite from that in 4_I, is explained below. What follows next is a description of the dynamic behavior of **4** observed upon warming.

Compound **4** displays three distinct dynamic processes. The first process equilibrates inequivalent butadiene exo protons, butadiene endo protons, butadiene methyls, and allyl syn and anti protons with each other in 4_I only (see Figure 5). Rapid rearrangement of 4_I to its enantiomer via an η^1-allyl transition state (bound at the unsubstituted carbon) would account for this. The $\Delta G^\ddagger$ of 39.4 ± 1.0 kJ/mol for this process [obtained from coalescence of endo protons (−71 °C), the exo protons (−72 °C), and the butadiene methyls (−78 °C)] compares very favorably to the barrier of 40.9 kJ/mol reported for η^3 to η^1 isomerization in Cp*Hf(1,1,2-Me_3allyl)Br_2.[17]

The second process allows for the interconversion of 4_I and 4_{II} (see Figure 6). This interconversion occurs with exchange of the exo protons of one isomer with the endo protons of the other ($\Delta G^\ddagger(4_I \rightarrow 4_{II})$ = 50.0 ± 1.0 kJ/mol; $\Delta G^\ddagger(4_{II} \rightarrow 4_I)$ = 49.7 ± 1.0 kJ/mol, estimated from the broadening of the Cp signals observed at −29.0 °C relative to the −94.0 °C static spectrum using the slow exchange approximation,[22] coalescence of the Cp signals occurred at −6 °C). Of the three common butadiene rearrangement modes only the flip or the slip mechanisms could accomplish this. It is important to note that the flip mechanism would also necessarily change the orientation of the butadiene ligand from prone to supine. The slip mechanism is unlikely given the static behavior of compound **3** mentioned earlier. Thus it is the flip mechanism, observed by Erker for compounds **1** and **2**, that is operative in this second dynamic process. The resulting supine butadiene orientation in 4_{II} is no longer hindered since the allyl ligand is now bound η^1. It is important to note that the barriers we observe for butadiene flip are approximately 35 kJ/mol less than those measured for compounds **1** and **2** in which butadiene flip is postulated to be accompanied by a simultaneous allyl rotation.[6] The barriers for butadiene flip in **4** are within 3 kJ of those measured for a series of

(21) Modeling calculations were carried out by using an extended version of Allinger's MM2 force field which includes transition metals. The programs were obtained from Serena Software Inc., P.O. Box 3076, Bloomington, IN 47402. The Hf-C bond distances were fixed at a somewhat long 2.70 Å for the allyl and butadiene ligands so as not to exaggerate van der Waals repulsions.

(22) (a) Emsley, J. W.; Feeney, J.; Sutcliffe, L. H. *High Resolution Nuclear Magnetic Resonance Spectroscopy*; Pergamon Press: Oxford, 1965; Vol. 1, p 481. (b) Anet, F. A. L. *J. Am. Chem. Soc.* **1964**, *86*, 458.

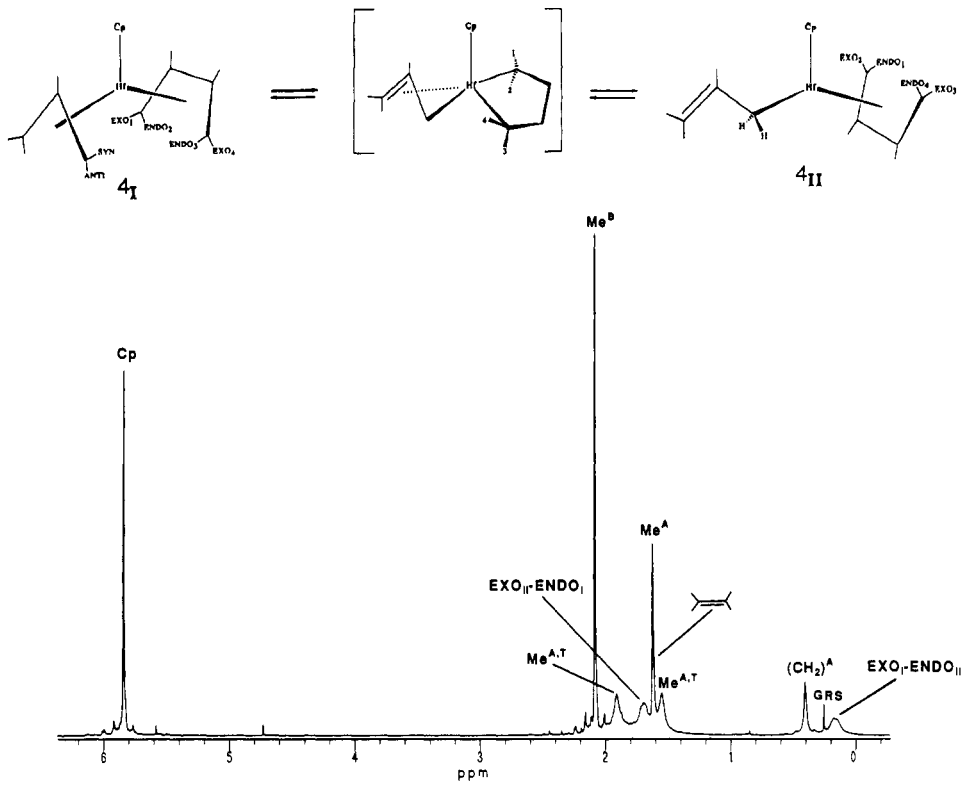

Figure 6. Second dynamic process, responsible for the interconversion of isomers 4_I and 4_{II}. The butadiene flip and allyl isomerization are not necessarily simultaneous as depicted (see the text). The ^1H NMR spectrum shown above was measured in toluene-d_8 at 70 °C (see Figure 4 caption for key to subscripts and superscripts). The terminal allyl methyl peaks are substantially broadened and coalesce at 95 °C due to a third, highest energy dynamic process. The 2,3-dimethyl-2-butene is due to the onset of thermal decomposition.

Cp_2Zr(butadiene) complexes in which butadiene flip is the only dynamic process that occurs.[6] Nevertheless, our data do not allow us to say if the butadiene flip that interconverts $4_I \leftrightarrow 4_{II}$ occurs simultaneously with the η^3 to η^1 allyl rearrangement that must also occur.

Finally, there is a third, highest energy, rearrangement process which exchanges terminal allyl methyl groups with each other [73.4 ± 1.0 kJ/mol, obtained from coalescence of the terminal allyl methyl signals (95 °C)]. Such methyl group exchange can be accomplished via a transition state in which the allyl ligand binds η^1 at the dimethylated carbon. This barrier is 34 kJ/mol higher than it is for similar rearrangement at the unsubstituted end of the allyl ligand (first barrier) as would be expected.[15] At temperatures above 70 °C compound **4** begins to decompose yielding free 2,3-dimethyl-2-butene (protenated allyl) and uncharacterizeable Hf species.

Isomers 4_I and 4_{II} are in rapid chemical equilibrium with each other at all measured temperatures. Whereas 4_I is the major isomer at low temperature, 4_{II} becomes the major isomer at higher temperatures. The equilibrium constant for $4_I \rightleftharpoons 4_{II}$ ($K = [4_{II}]/[4_I]$) was determined at 20 °C intervals from relative Cp peak areas up to the point where exchange was rapid on the NMR time scale [K = 0.085 (−94 °C); 0.218 (−80 °C); 0.428 (−60 °C); 0.834 (−40 °C); 1.317 (−20 °C)]. A van't Hoff plot of ln (K) versus $1/T$ was linear and a least-squares determined slope gave a calculated $\Delta H(4_I \rightarrow 4_{II})$ of 13.6 kJ/mol.

Conclusions

Ligand methylation has a profound effect on the structural and dynamic properties of CpHf(allyl)(butadiene) complexes. The orientation (supine or prone) of the open π ligands is determined predominantly by the nonbonded repulsions involving the methyl groups on these ligands. Whereas a simultaneous allyl rotation is postulated to accompany a butadiene flip in compounds **1** and **2**, no such allyl rotation occurs for **4**. Such an allyl rotation would deliver **4** into the supine–supine configuration, shown by molecular mechanics calculations to be highly unfavorable. Instead, **4** rearranges by a butadiene flip mechanism which is preceeded by a more rapid allyl η^3 to η^1 isomerization.

Acknowledgment is made to the National Science Foundation RUI program (Grant No. CHE-8800845), the National Science Foundation REU program (Grant No. CHE-8804803), and to the Camille and Henry Dreyfus Foundation Teacher–Scholar Program.

Supplementary Material Available: Tables of hydrogen atom coordinates and anisotropic thermal parameters for **3** (Tables III and IV) (2 pages); a listing of observed and calculated structure factors for **3** (Table V) (5 pages). Ordering information is given on any current masthead page.